



Published in final edited form as:

Nat Chem. 2019 November ; 11(11): 1034–1040. doi:10.1038/s41557-019-0344-4.

Regio- and Diastereoselective Intermolecular [2+2] Cycloadditions Photocatalyzed by Quantum Dots

Yishu Jiang¹, Chen Wang², Cameron R. Rogers¹, Mohamad S. Kodaimati¹, Emily A. Weiss^{1,*}

¹Department of Chemistry, Northwestern University, 2145 Sheridan Rd., Evanston, IL 60208-3113

²Department of Chemistry and Biochemistry, Queens College, 65-30 Kissena Boulevard, Flushing, NY 11367

Abstract

Light-driven [2+2] cycloaddition is the most direct strategy to build tetrasubstituted cyclobutanes, core components of many lead compounds for drug development. Significant advances in the chemoselectivity and enantioselectivity of [2+2] photocycloadditions have been made, but exceptional and tunable diastereoselectivity and regioselectivity (head-to-head vs. head-to-tail adducts), required for synthesis of bioactive molecules, have not yet been achieved. Here we show that colloidal quantum dots (QDs) serve as visible-light chromophores, photocatalysts, and reusable scaffolds for homo- and hetero-intermolecular [2+2] photocycloadditions of 4-vinylbenzoic acid derivatives, including aryl-conjugated alkenes, with up to 98% switchable regioselectivity and 98% diastereoselectivity for the previously minor *syn*-cyclobutane products, including the *syn*-head-to-tail cyclobutane, which has never before been accessed as the major product of a hetero-photocycloaddition. Transient absorption spectroscopy confirms that our system is the first example of catalysis triggered by triplet-triplet energy transfer from a QD. The precisely controlled triplet energy levels of QD photocatalysts facilitate efficient and selective heterocoupling, a major challenge in direct cyclobutane synthesis.

Light-driven [2+2] cycloadditions^{1–5}, simple routes to complex, biologically relevant tetrasubstituted cyclobutanes^{6–8}, follow several possible excited-state routes. Those that proceed through the triplet excited state of the reagent olefin are advantageous because (i) their scope is not limited by the electrochemical potentials of the substrate, (ii) triplets have long enough lifetimes to mediate *intermolecular* cycloadditions, and (iii) triplets are accessible with visible light through excitation of a triplet sensitizer, such as a transition metal complex or organic chromophore⁹, followed by triplet-triplet energy transfer (TT

Users may view, print, copy, and download text and data-mine the content in such documents, for the purposes of academic research, subject always to the full Conditions of use:http://www.nature.com/authors/editorial_policies/license.html#terms **Reprints and permissions information** is available at <http://www.nature.com/reprints>.

*corresponding author. e-weiss@northwestern.edu. **Correspondence and requests for materials** should be addressed to E.A.W. **Author Contributions:** Y.J., C.W., C.R.R., and E.A.W. conceived the project and contributed to experimental design and analysis. Y.J. and C.W. conducted the optimization and control studies described in the supplementary materials. C.R.R. synthesized the substrates and analyzed the 2D NMR data. M.S.K. performed the computational studies. All authors contributed to the writing and editing of the manuscript.

Competing interests The authors declare no competing interests.

Supplementary Information is linked to the online version of the paper at www.nature.com/nature.

EnT). The TT EnT strategy minimizes deleterious side-reactions and has resulted in high-yield intra- and intermolecular [2+2] photocycloadditions of quinolone^{1,10}, cinnamate and derivatives^{11,12}.

Pioneering work of Bach, Meggers, Yoon and others has demonstrated enantioselective intermolecular [2+2] photocycloadditions in the presence of hydrogen bonding templates^{1,2}, chiral secondary amines³, chiral ligands of molecular catalysts⁴ and Lewis-acid co-catalysts⁵. Outstanding challenges include the competing fast cis/trans isomerization pathway of the substrates, and achieving selectivities for a particular regioisomer or diastereomer of the coupled product and for homo- vs. heterocoupling within a mixture of reactive olefins – the latter a priority because cyclobutane natural products and related compounds predominantly comprise two distinct olefins¹³. First, the *anti* diastereomer of the cyclobutyl product is sterically favored in untemplated reactions but the preference is often not significant enough to achieve efficient discrimination¹⁴. The *syn* diastereomer has been accessed only using templates that interact with substrates through covalent and non-covalent linkages, and through solid-state reactions. The syntheses of covalent scaffolds like paracyclophane¹⁵ – and, more importantly, the reactions used to cleave the addition product from the template – are however complex and often low-yielding, whereas non-covalent scaffolds (usually involving hydrogen bonds)¹⁶ have a very limited substrate scope and are often not rigid enough to template intermolecular reactions effectively. The solid-state reactions are a synthetically simpler approach to accessing *syn* diastereomers¹⁷, but do not offer a straightforward way to sensitize the reaction with visible light, or a way to achieve chemoselectivity and enantioselectivity.

Second, the distribution of head-to-head (HH) vs. head-to-tail (HT) regioisomers of [2+2] cycloadditions is highly dependent on the relative stability of the corresponding triplet biradical intermediates and therefore difficult to control extrinsically. Most HT homocoupled products are achieved through solid state reactions¹⁸, or through a select few liquid state methods that use templates or molecular cages^{19,20}, but regioselective HT heterocoupled products have not been accessed with these methods.

Third, selective heterocoupling is challenging to achieve even with a template or a solid-state reaction, because it requires selective co-localization of two different substrates. Reported examples are limited to coupling of two very similar, highly symmetric substrates, such as two monosubstituted stilbenes; this reaction has no regioselectivity²¹. Prior to this work, *syn*-HT heterocoupled products, the class of tetrasubstituted cyclobutanes that serve as scaffolds for many bioactive molecules, had never been formed as major products of a [2+2] photocycloaddition. In fact, there were no examples of tunable regioselectivity for any hetero-intermolecular [2+2] photocycloadditions. A strategy for extrinsic control of the configuration of the cyclobutane product is needed to counter the preferences driven by steric and electronic characteristics of the substrates.

Here, we use colloidal CdSe quantum dots (QDs) as visible light absorbers, triplet exciton donors, and self-assembly scaffolds to drive homo- and hetero-intermolecular [2+2] photocycloadditions of 4-vinylbenzoic acid derivatives. CdSe QDs donate energy to triplet states of organic molecules from triplet-like excitonic “dark” states, which lie <20 meV

below their optically active “bright states”^{22–25}. A QD’s triplet energy is tunable *via* size-dependent quantum confinement; here we adjust the size of the QD to selectively sensitize only one reagent olefin within a mixture, and thereby achieve efficient *hetero*-intermolecular couplings. The QD catalytic systems exhibit up to 98% switchable (between HH and HT) regioselectivity with up to 98% diastereoselectivity for the previously minor *syn*-HH or *syn*-HT configurations of the adducts, including those made from challenging stilbene derivatives (Figs. 1a,b). With one exception, highlighted below, the diastereomeric ratios (d.r.) we achieve are a factor of 5–10 higher than those reported with all other triplet sensitizers for similar systems^{11,12}.

Results and Discussion

The Supplementary Information (SI) contains all details of synthesis and chemical analysis. The QDs do not etch, aggregate, or otherwise degrade for at least three 48 h reaction cycles (Fig. 1c). We readily separate the QD catalysts from reaction mixtures through addition of MeOH and centrifugation, and reuse them with no detectable decline in catalytic activity, Supplementary Table 1. No reactions occurred without QDs or without illumination, Supplementary Table 2. Through transient absorption spectroscopy, we observe coincident decays of the photoexcited electron and hole of the QD when the substrate is present, Fig. 1d. This result indicates that they are extracted from the QD as an electron-hole pair, and that the reaction is EnT-initiated rather than redox-initiated (and specifically TT EnT-initiated, since the singlet excited states of all substrates are too high-energy to access). The coupling yields of all reactions are 10x lower when we do not functionalize both substrates with carboxylate groups to reversibly bind to the QD (Supplementary Scheme 1), indicating that the reaction occurs at the surface of the particle. Carboxylates are “medium-strength” ligands for the surfaces of CdSe ($k_{\text{self-exchange}} \sim 500 \text{ s}^{-1}$)²⁶, so coupled products desorb from the QD surface to make room for new substrates.

Table 1 shows a set of [2+2] photocycloadditions of 4-vinylbenzoic acid and derivatives that demonstrate the activity and diastereoselectivity of our QD photocatalyst when directly compared to tris(2,2'-bipyridine)ruthenium(II) (Ru(bpy)₃²⁺) or tris(2-phenylpyridinato)iridium(III) (Ir(ppy)₃), which have been used to perform similar reactions^{11,12}. The QD systems generate *syn* products with d.r. > 30:1, while the molecular complexes prefer *anti* products with much lower selectivity (d.r. < 3:1). The *syn* stereochemistry of the QD products is verified by X-ray crystallography of **8** (Supplementary Fig. 4) and Nuclear Overhauser Spectroscopy (NOESY NMR) of all products. For the heterocoupling of **3** and either **1** or **2**, the QDs produce *syn* products with d.r. > 40:1, while the molecular complexes prefer *anti* products with d.r. < 2:1. For the stilbene derivatives **4** - **7**, cycloadditions catalyzed by the molecular complexes do not occur with measureable yield, probably because of the known fast *cis/trans* isomerization of the excited-state substrates; we indeed observe a high concentration of *cis* isomers in the crude reaction mixtures after illumination. QDs, in contrast, photocatalyze reactions with excellent coupling yields, either, we propose, by accelerating the coupling step through co-localization of substrates or by slowing the isomerization by tethering the substrates on the QD surface.

The selective production of the kinetically disfavored *syn* configuration by the QDs, even in the case of two different coupling partners, is remarkable considering that the only templating chemistry is the reversible association of a carboxylate on the substrate with Cd²⁺ on the QD surface. The ability of intermolecular π - π interactions among rigid olefins to promote *syn* stereochemistry in solid-state reactions²⁷⁻²⁹ suggests that these same non-covalent interactions are responsible for the *syn* selectivity in the QD system, Fig. 1a.

Figure 2 illustrates the role of tunable QD size in achieving heterocoupling (over homocoupling) through selective TT EnT. The difficulty in controlling competition between homo- and heterocoupling has limited the scope of previous heterocouplings to substrates with large triplet energy differences. In this case, the triplet energies of **1** and **3** (2.25 eV and 2.51 eV respectively) are close enough such that Ir(ppy)₃ indiscriminately sensitizes both substrates (Fig. 3B), resulting in 23% of the substrate **3** producing the undesired homocoupled product **9**. In contrast, 1.4 nm CdSe QDs perform selective TT EnT to **1** without sensitizing **3**, yielding highly efficient heterocoupling (92% yield of **14**) with <5% of **3** participating in homocoupling. The comparatively unselective performance of the higher-energy 1.0 nm CdSe QDs illustrates that selective energetic overlap with a specific substrate is the key to efficient heterocoupling.

Figure 3 demonstrates the >90% tunable regioselectivity achievable for hetero-[2+2] photocycloadditions using our QD system. Most notably this system produces the disfavored heterocoupled HT regioisomers **25**, **27** and **30**. For untemplated reactions, *i.e.*, those photosensitized by Ir(ppy)₃ or by QDs when one substrate does not have a carboxylic acid substituent (gray shaded area), formation of the HH regioisomer is strongly favored through benzylic stabilization of the corresponding 1,4-diradical intermediate. In order to access the *syn*-HT heterocoupled products **25**, **27** and **30**, which have never been formed as a major product of [2+2] photocycloaddition, we tuned the regioselectivity of the QD-catalyzed reactions through the position of the carboxylate on each substrate (Fig. 3a). For coupling of **1**, **4**, **6** and **2**, we achieve perfect HH regioselectivity with no HT products detected. When the carboxylate moiety is relocated to the opposite side of the substrate (**5** vs. **4**, **7** vs. **6**, **22** vs. **1**), the observed regioselectivity of the QD catalyst switches entirely, providing the HT product for the heterocoupling of **5**, **7** and **2** with r.r. >40:1 and **22** and **2** with r.r. >10:1. The *syn* diastereoselectivity is preserved in these regioselective reactions: the heterocoupled products **24** - **28** have d.r. >37:1 and product **30** has d.r. >10:1.

The Ir(ppy)₃ sensitizer produces the HH configuration as the major product regardless of whether **2** is coupled with **22** or **1** and the weak preference for the *anti* diastereomer remains in products **29** and **31** with d.r. up to 5:1. The loss of regioselectivity upon removing the carboxylate from one of the substrates (**23**) shows that the QD system achieves regioselective heterocoupling through pre-arrangement of substrates at the QD surface, a manner entirely independent of electronics of the reactive olefin. Moreover, the heterocoupling of stilbenes **4** - **7** with **2** by molecular substrates produces no measureable yield because of the same competing isomerization pathway described in reference to Table 1.

An examination of the unusually poor performance of the QD-catalyzed reaction between **22** and **2** shows that lower overall yield and selectivity is not due to side products (72% of the remaining yield can be accounted for by starting material), but, we believe, is limited by the location of triplet acceptor orbitals of the substrate (Fig. 3b). For **1**, the transition to the triplet excited state ($S_0 \rightarrow T_1$) has good spatial overlap with the binding group of the substrate, and therefore good electronic coupling with the QD. For **22**, there is a spatial gap between the QD surface and the triplet density; this gap makes TT EnT inefficient.

In summary, we have described a new and powerful approach to selective [2+2] photocycloadditions, and simultaneously presented the first example of catalysis triggered by triplet-triplet energy transfer from a quantum dot. By inducing self-assembly of substrate molecules through reversible association with the QD surface, we have accessed excellent diastereoselectivity and tunable regioselectivity – including previously inaccessible *syn*-HT photo-adducts – the first example of either selectivity type using the QD ligand shell, and the first examples of tunably regioselective hetero-intermolecular [2+2] photocycloadditions. The precisely controlled triplet energy levels of QD photocatalysts facilitate efficient and selective heterocoupling. Overall, QDs present a strategy for extrinsic control of the configuration of the cyclobutane product that counters the stereo-electronic preferences of the substrates, and have great potential to enhance any reaction that proceeds through a triplet excited state, including metal complex-catalyzed reactions. Improvement of the quantum efficiencies (moles product per incident photon) could be achieved by tuning the relative excited state energies of the QD and molecular substrate such that back-TT EnT is not competitive with the forward process³⁰.

Data availability statement

Crystallographic data for the structures reported in this Article have been deposited at the Cambridge Crystallographic Data Centre, under deposition numbers CCDC 1900373. Copies of the data can be obtained free of charge via <https://www.ccdc.cam.ac.uk/structures/>. All other data supporting the findings of this study are available within the Article (Figures 1–3 and Table 1) and its Supplementary Information (Supplementary Tables 1–8, Supplementary Scheme 1, Supplementary Figures 1–4, Supplementary Sections L, M), or from the corresponding author upon reasonable request.

Supplementary Material

Refer to Web version on PubMed Central for supplementary material.

Acknowledgements

The authors thank Profs. Regan Thomson and Andrew Lee for helpful discussions. Research primarily supported by through the Air Force Office of Scientific Research (grant 9550-17-1-0271) (synthesis, photocatalysis, analytical chemistry), and by the Center for Bio-Inspired Energy Science, an Energy Frontier Research Center funded by the U.S. Department of Energy (DOE), Office of Science, Basic Energy Sciences (BES), under Award # DE-SC0000989 (calculations). C.R.R. thanks the International Institute for Nanotechnology at Northwestern University for a fellowship. This work made use of the IMSERC at Northwestern University, which has received support from the NIH (1S10OD012016-01 / 1S10RR01907101A1); Soft and Hybrid Nanotechnology Experimental (SHyNE) Resource (NSF ECCS-1542205); the State of Illinois and International Institute for Nanotechnology (IIN).

References

1. Alonso R & Bach T A Chiral Thioxanthone as an Organocatalyst for Enantioselective [2+2] Photocycloaddition Reactions Induced by Visible Light. *Angew. Chem* 126, 4457–4460.
2. Maturi MM & Bach T Enantioselective Catalysis of the Intermolecular [2+2] Photocycloaddition between 2-Pyridones and Acetylenedicarboxylates. *Angew. Chem. Int. Ed* 53, 7661–7664.
3. Hörmann FM, Chung TS, Rodriguez E, Jakob M & Bach T Evidence for Triplet Sensitization in the Visible-Light-Induced [2+2] Photocycloaddition of Eniminium Ions. *Angew. Chem. Int. Ed* 57, 827–831.
4. Hu N et al. Catalytic Asymmetric Dearomatization by Visible-Light-Activated [2+2] Photocycloaddition. *Angew. Chem. Int. Ed* 57, 6242–6246.
5. Blum TR, Miller ZD, Bates DM, Guzei IA & Yoon TP Enantioselective Photochemistry through Lewis Acid-Catalyzed Triplet Energy Transfer. *Science* 354, 1391–1395.
6. Dembitsky VM Bioactive cyclobutane-containing alkaloids. *J. Nat. Med* 62, 1–33. [PubMed: 18404338]
7. Lee-Ruff E & Mladenova G Enantiomerically Pure Cyclobutane Derivatives and Their Use in Organic Synthesis. *Chem. Rev* 103, 1449–1484.
8. Tsai I-L et al. New Cytotoxic Cyclobutanoid Amides, a New Furanoid Lignan and Anti-Platelet Aggregation Constituents from Piper Arborescens. *Planta Med.* 71, 535–542. [PubMed: 15971125]
9. Prier CK, Rankic DA & MacMillan DWC Visible Light Photoredox Catalysis with Transition Metal Complexes: applications in Organic Synthesis. *Chem. Rev* 113, 5322–5363. [PubMed: 23509883]
10. Tröster A, Alonso R, Bauer A & Bach T Enantioselective Intermolecular [2 + 2] Photocycloaddition Reactions of 2(1H)-Quinolones Induced by Visible Light Irradiation. *JACS* 138, 7808–7811.
11. Lei T et al. General and Efficient Intermolecular [2+ 2] Photodimerization of Chalcones and Cinnamic Acid Derivatives in Solution through Visible-Light Catalysis. *Angew. Chem. Int. Ed* 56, 15407–15410.
12. Pagire SK, Hossain A, Traub L, Kerres S & Reiser O Photosensitized Regioselective [2+ 2]-Cycloaddition of Cinnamates and Related Alkenes. *Chem. Commun* 53, 12072–12075.
13. Gutekunst WR & Baran PS Applications of C–H Functionalization Logic to Cyclobutane Synthesis. *J. Org. Chem* 79, 2430–2452.
14. Poplata S, Tröster A, Zou Y-Q & Bach T Recent Advances in the Synthesis of Cyclobutanes by Olefin [2+2] Photocycloaddition Reactions. *Chem. Rev* 116, 9748–9815. [PubMed: 27018601]
15. Zitt H, Dix I, Hopf H & Jones P 4,15-Diamino[2.2]paracyclophane, a Reusable Template for Topochemical Reaction Control in Solution. *Eur. J. Org. Chem* 2002, 2298–2307.
16. Bassani DM, Darcos V, Mahony S & Desvergne J-P Supramolecular Catalysis of Olefin [2 + 2] Photodimerization. *JACS* 122, 8795–8796.
17. Elacqua E et al. A Supramolecular Protecting Group Strategy Introduced to the Organic Solid State: Enhanced Reactivity through Molecular Pedal Motion. *Angew. Chem. Int. Ed* 51, 1037–1041.
18. Zhang P et al. Enantioselective Biomimetic Total Syntheses of Katsumadain and Katsumadain C. *Org. Lett* 14, 162–165. [PubMed: 22148865]
19. Skiredj A et al. Spontaneous Biomimetic Formation of (±)-Dictazole B under Irradiation with Artificial Sunlight. *Angew. Chem. Int. Ed* 53, 6419–6424.
20. Pattabiraman M, Natarajan A, Kaliappan R, Mague JT & Ramamurthy V Template Directed Photodimerization of Trans-1, 2-bis (n-pyridyl) Ethylenes and Stilbazoles in Water. *Chem. Commun*, 4542–4544.
21. Bu ar D-K, Sen A, Mariappan SVS & MacGillivray LRA [2+2] Cross-Photodimerisation of Photostable Olefins via a Three-Component Cocrystal Solid solution. *Chem. Commun* 48, 1790–1792.
22. Mongin C, Garakyaraghi S, Razgoniaeva N, Zamkov M & Castellano FN Direct Observation of Triplet Energy Transfer from Semiconductor Nanocrystals. *Science* 351, 369–372. [PubMed: 26798011]

23. Huang Z, Simpson DE, Mahboub M, Li X & Tang ML Ligand Enhanced Upconversion of Near-Infrared Photons with Nanocrystal Light Absorbers. *Chem. Sci* 7, 4101–4104. [PubMed: 30155053]
24. Efros AL et al. Band-edge Exciton in Quantum Dots of Semiconductors with a Degenerate Valence Band: Dark and Bright Exciton States. *Phys. Rev. B* 54, 4843.
25. Nirmal M et al. Observation of the “Dark Exciton” in CdSe Quantum Dots. *Phys. Rev. Lett* 75, 3728. [PubMed: 10059712]
26. Fritzing B, Capek RK, Lambert K, Martins JC & Hens Z Utilizing Self-Exchange to Address the Binding of Carboxylic Acid Ligands to CdSe Quantum Dots. *J. Am. Chem. Soc* 132, 10195–10201.
27. MacGillivray LR et al. Supramolecular Control of Reactivity in the Solid State: From Templates to Ladderanes to Metal–Organic Frameworks. *Acc. Chem. Res* 41, 280–291. [PubMed: 18281948]
28. Ito Y *Solid-state Organic Photochemistry of Mixed Molecular Crystals*. Vol. 3 (Dekker: New York, 1999).
29. Natarajan AB, B. R in *Supramolecular Photochemistry. Controlling Photochemical Processes* (ed. Ramamurthy V, Inoue Y) 175–228 (Wiley, 2011).
30. Mongin C, Moroz P, Zamkov M & Castellano FN Thermally Activated Delayed Photoluminescence from Pyrenyl-Functionalized CdSe Quantum Dots. *Nature Chem.* 10, 225. [PubMed: 29359748]

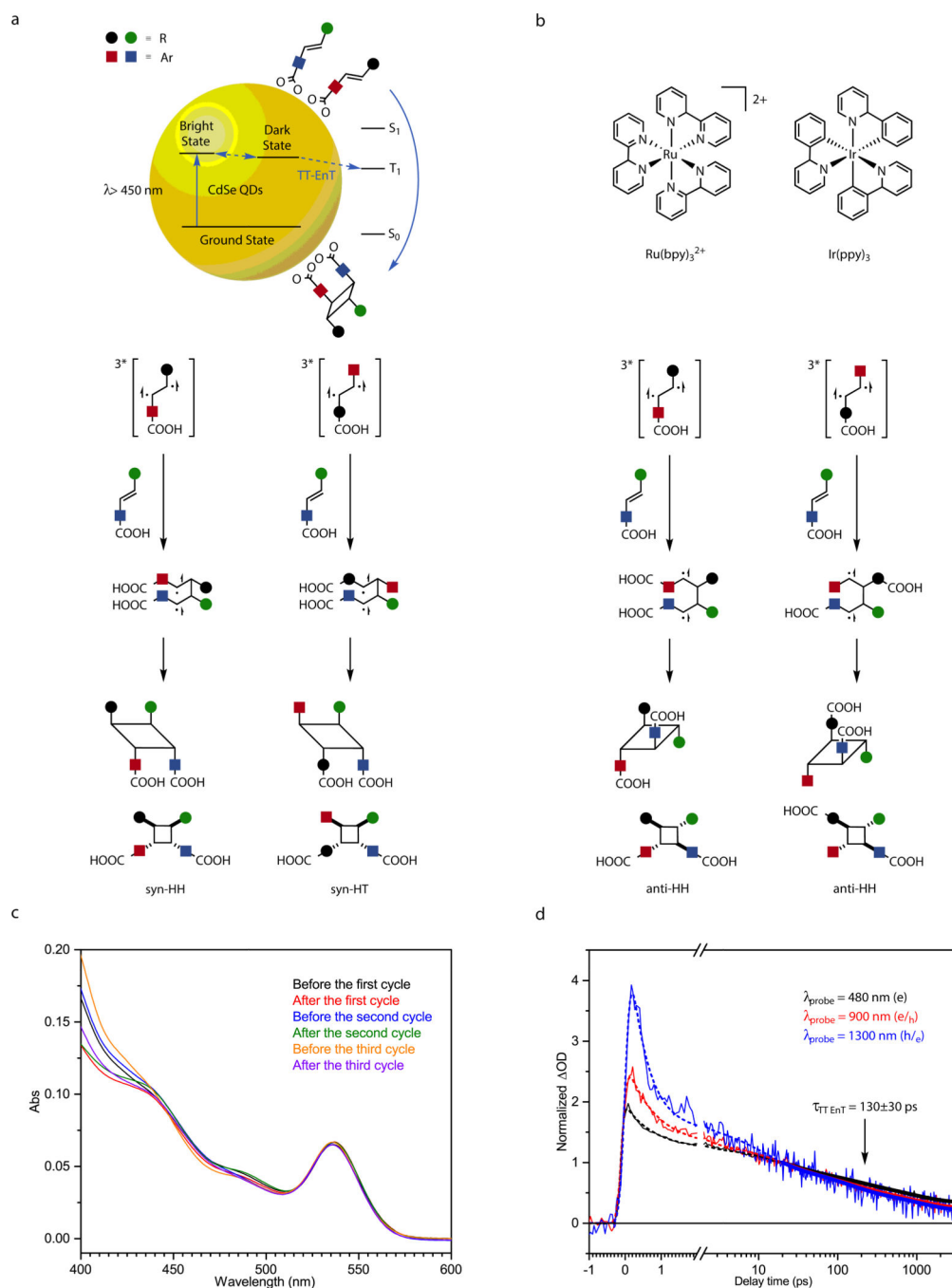


Fig. 1. Sensitization via the QD Photocatalyst and Mechanisms of Selectivity.

a, Sensitization of the triplet excited state of the substrate (T_1) through TT-EnT from CdSe QDs, and schematic representation of *syn*-HH or *syn*-HT selectivity of QDs. A proposed mechanism of the route to each diastereomer is shown in Supplementary Scheme 2. The best regioselectivity is achieved with molecules where the black circle represents an aromatic group (Ar). **b**, Chemical structures of the molecular sensitizers, and the mechanism of *anti*-HH preference of reactions driven by these molecules. **c**, Ground state absorption spectra of a mixture of CdSe QDs (radius = 1.4 nm) and **1** in THF, before and after three 48-h

illumination cycles. The differences between spectra at $\lambda < 450$ nm are due to consumption of **1**. **d**, Decay dynamics of the exciton in CdSe QDs mixed with 250 eq of **1** in THF, upon photoexcitation at 470 nm, monitored at three wavelengths: 480 nm (pure electron dynamics), 900 nm (primarily electron dynamics), and 1300 nm (primarily hole dynamics). Electrons and holes decay with a time constant of 130 ± 30 ps (where the error bar is the standard error) in the presence of **1**; this time constant is absent if **1** is not present, see Supplementary Fig. 1, Supplementary Table 3. The cyclic voltammetry of **1** and the band-edge energies of the CdSe QDs are in the SI, Supplementary Fig. 4. “OD” \equiv optical density.

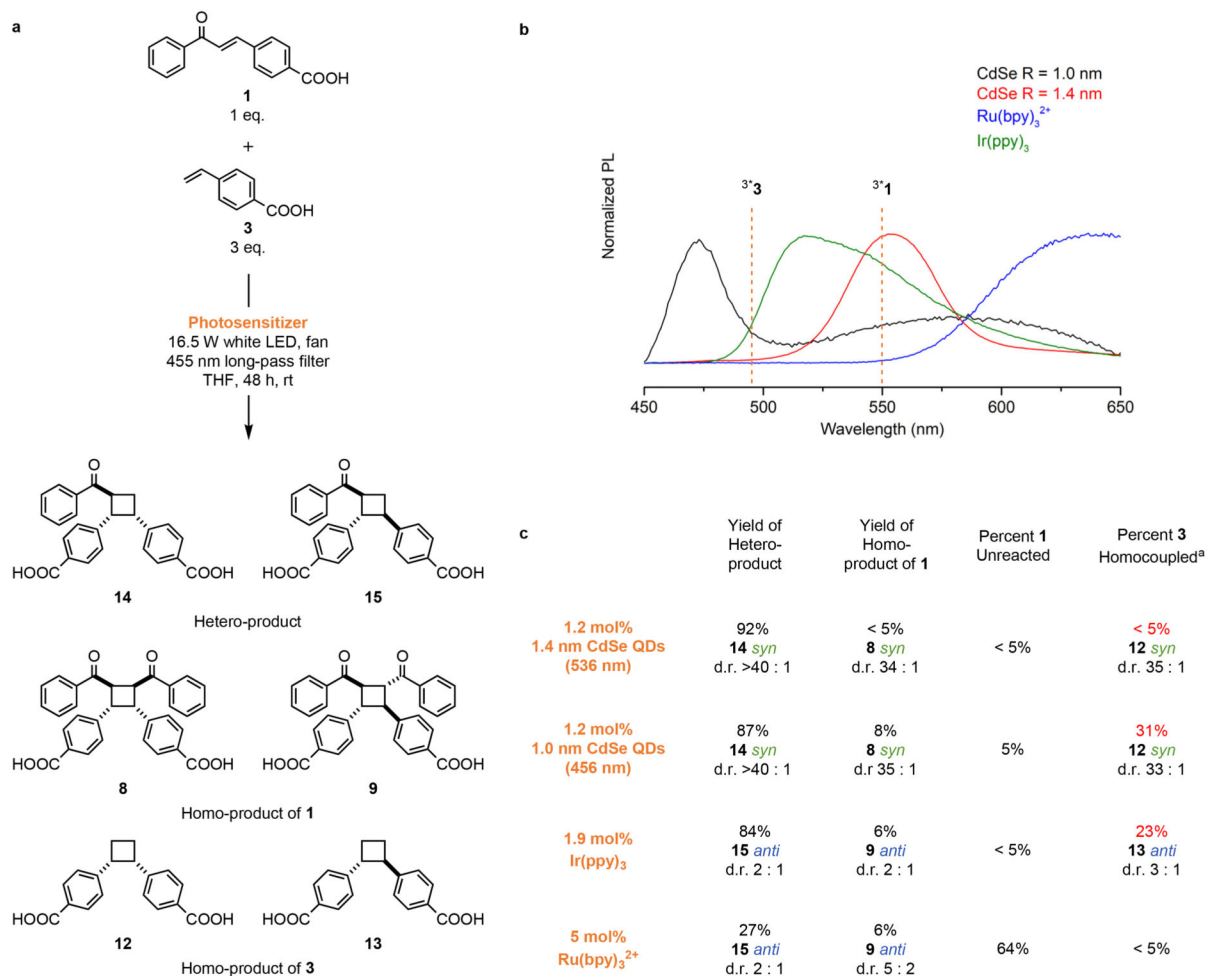


Fig. 2. Control of Homo- vs. Heterocycloaddition with QD Size.

a. Conditions for and possible products of [2+2] photocycloadditions of **1** and **3**. **b.** Emission spectra of four photosensitizers, compared with the triplet energies of substrates **1** and **3**, determined from phosphorescence spectra and calculations, see the SI. PL \equiv photoluminescence. **c.** Product distributions from reaction mixtures with the four photosensitizers. The yields listed are for the regioisomers indicated (drawn in **a**); the remaining mass is exclusively starting materials and the *cis*-isomer of **1** for the QD systems, and the same plus minor unidentified side products for the moleculecatalyzed reactions, see the SI. ^aThe yields in red are calculated in reference to substrate **3**, which was added in excess.

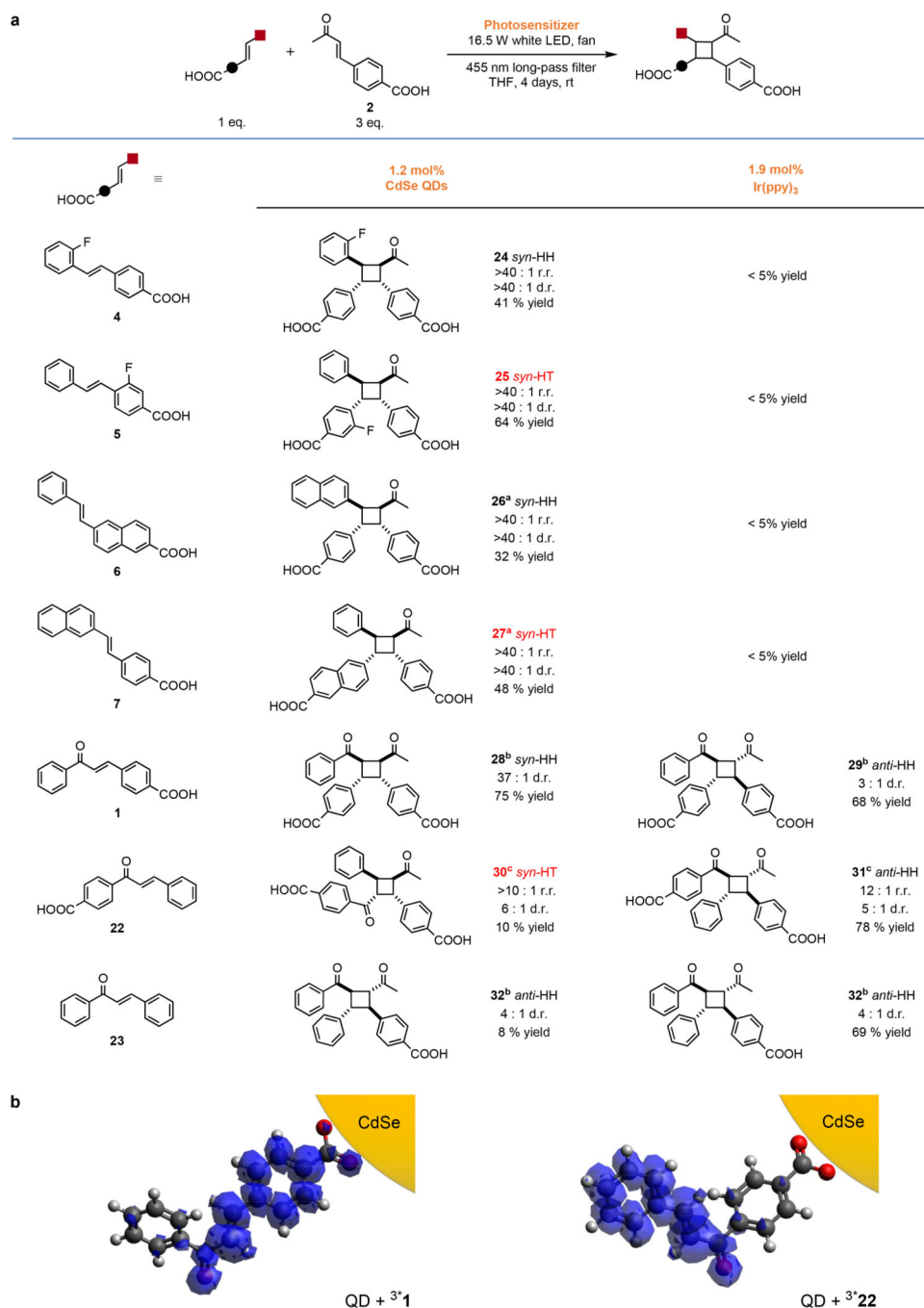


Fig. 3. Regioselectivity through Substrate Affinity for the QD Surface.

a. Conditions and product distributions for the [2+2] photocycloadditions of **2** and **1**, **4** to **7**, **22** or **23**. When **2** is coupled with **23**, with no carboxylic acid linker, the distribution of regioisomer products matches that of Ir(ppy)₃. The yields listed for QD reactions are isolated yields for the diastereomers drawn (the major products), except for the reaction with the control substrate **23**. The yields listed for Ir(ppy)₃ and Ru(bpy)₃²⁺ systems are the NMR yields of the regioisomers drawn. The remaining mass of the coupling of **2** with **22** is starting materials and their *cis*-isomers (>72%), the HH regioisomer, and the

homocycloaddition products of both substrates for the QD system, and is the same plus minor unidentified side products for the Ir(ppy)₃ system, see the SI. ^aReactions were catalyzed with 2.4 mol% QDs. ^bReactions were illuminated for 2 days. ^cThe reaction was illuminated with a blue LED. **b**, Transition densities for the first triplet excited states of **1** and **22** calculated using time-dependent density functional theory (TD-DFT).

Author Manuscript

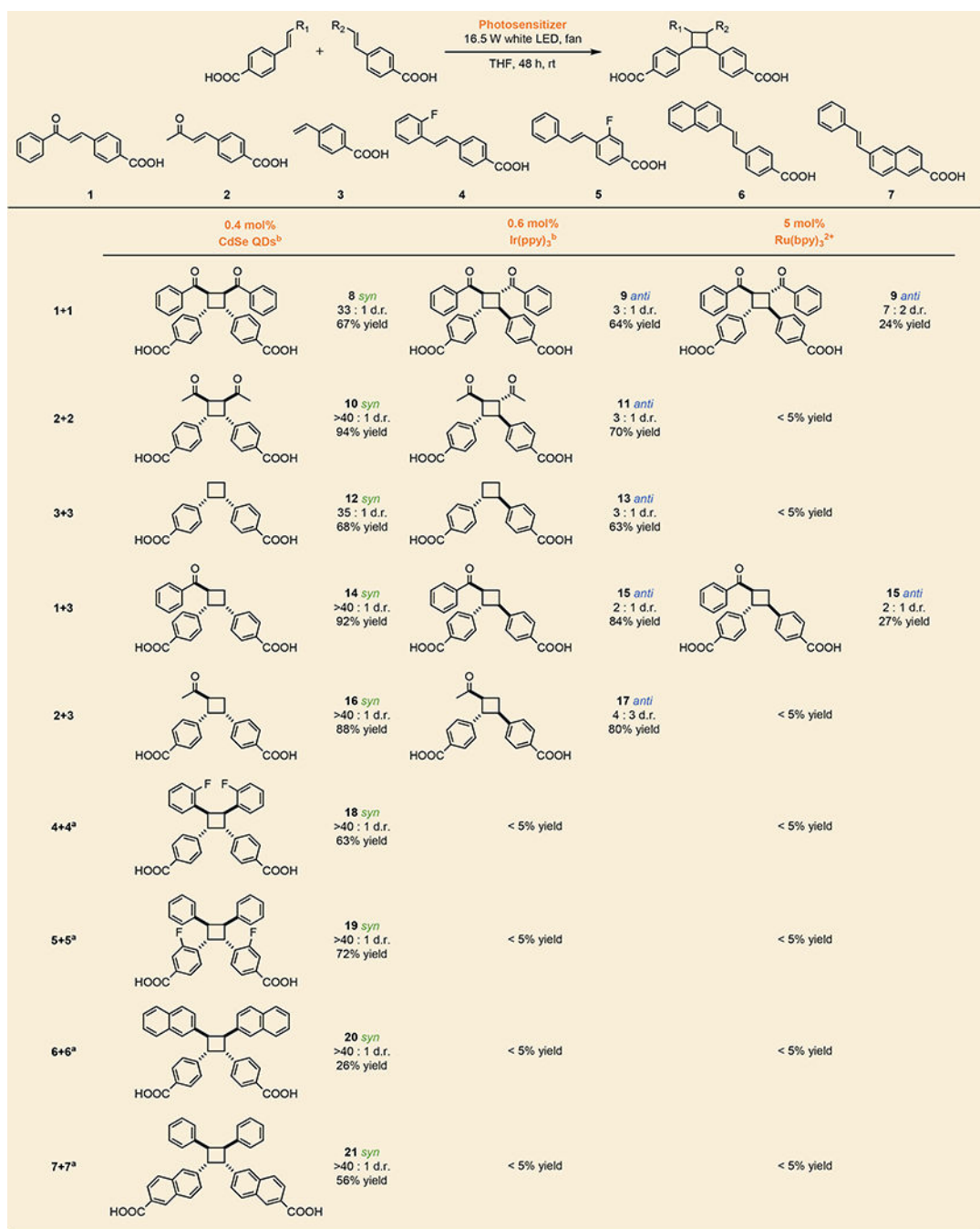
Author Manuscript

Author Manuscript

Author Manuscript

Table 1 |

Diastereoselectivity through Pre-organization on the QD Surface.



The triplet spectra of **1** and **2** shown in Supplementary Fig. 2. The yields listed are the isolated yields of the diastereomers drawn for QD systems (remaining mass=starting material and its cis-isomer; zero HT product) and the NMR yields of the regioisomers drawn for Ir(ppy)₃ and Ru(bpy)₃²⁺ systems (remaining mass=starting material and its cis-isomer, minor unidentified side products), see the SI. Reactions of **1** were illuminated with >455 nm light so as not to excite the substrate directly.

^aReactions were illuminated for 4 days.

^bListed loadings are for homocycloadditions; catalyst loadings for heterocycloadditions are 1.2 mol% QDs and 1.9 mol% molecular sensitizers.

Author Manuscript

Author Manuscript

Author Manuscript

Author Manuscript